

---

# A Fast Foveated Fully Convolutional Network Model for Human Peripheral Vision

---

**Lex Fridman**  
MIT  
fridman@mit.edu

**Benedikt Jenik**  
MIT  
bjenic@mit.edu

**Shaiyan Keshvari**  
MIT  
shaiyan@mit.edu

**Bryan Reimer**  
MIT  
reimer@mit.edu

**Christoph Zetsche**  
University of Bremen  
zetsche@informatik.uni-bremen.de

**Ruth Rosenholtz**  
MIT  
rruth@mit.edu

## Abstract

Visualizing the information available to a human observer in a single glance at an image provides a powerful tool for evaluating models of full-field human vision. The hard part is human-realistic visualization of the periphery. Degradation of information with distance from fixation is far more complex than a mere reduction of acuity that might be mimicked using blur with a standard deviation that linearly increases with eccentricity. Rather, behaviorally-validated models hypothesize that peripheral vision measures a large number of local texture statistics in pooling regions that overlap, grow with eccentricity, and tile the visual field. We propose a “foveated” variant of a fully convolutional network that approximates one such model. Our approach achieves a 21,000 fold reduction in average running time (from 4.2 hours to 0.7 seconds per image), and statistically similar results to the behaviorally-validated model.

## 1 Introduction and Related Work

In the fovea (i.e., the central rod-free area of the retina, approximately  $1.7^\circ$  diameter), recognition is relatively robust and effortless. However, more than 99% of visual field lies outside the fovea, here referred to as the periphery. Peripheral vision has considerable loss of information relative to the fovea. This begins at the retina, which employs variable spatial resolution to get past the bottleneck of the optic nerve. However, it does not end there, but continues with neural operations in visual cortex. Reduced peripheral acuity has only a tiny effect, compared with peripheral vision’s sensitivity to clutter, known as visual crowding (discussed in more detail in §1.2). Unlike acuity losses, which impact only tasks relying on quite high spatial frequencies, crowding occurs with a broad range of stimuli [20]. It is ever-present in real-world vision, in which the visual system is faced with cluttered scenes full of objects and diverse textures. Crowding constrains what we can perceive at a glance, which in turn constrains visual performance more generally.

In prior work, researchers visualized both reduced acuity and visual crowding using foveated texture synthesis techniques that generate new image samples that have the same texture statistics in a large number of overlapping “pooling” regions [8, 24]. Such visualizations facilitate intuitions about peripheral vision, e.g. for design, and also have enabled testing models of peripheral vision. The underlying model has been shown to predict performance at a number of peripheral and full-field vision tasks [2, 12, 13, 25, 32]. However, generating each synthesis can take a number of hours, limiting the utility of this technique.



(a) Original  $512 \times 512$  pixel image.



(b) Foveated image with fixation on  $(256, 256)$ .

Figure 1: Example “foveated” image. Given an original image (a), the foveated image provides a visualization of the information available from a single glance (b) assuming the two subfigures are 14.2 inches away from the observer on a printed page (2.6 inches in height and width) and the observer’s eyes are fixated at the center of the original image. By selecting a new model fixation, one can similarly get predictions for that fixation. Any part of the image that appears clearly in (b) is predicted to be easy to perceive when fixating at the center of (a). The stripes in the flag are clear. The cat is clearly identifiable as such, and clearly sits next to a book. The pictures within the book are not predicted to have a clear organization, given the modeled fixation. The image in this example comes from the dataset used in the paper.

In this work, we propose a Foveated Fully Convolution Network (FFCN) architecture for end-to-end learning of the foveation task. The primary goal of this approach is to reduce the running time of generating a human-realistic visualization of peripheral vision from hours to milliseconds while maintaining reasonable consistency with the behaviorally-validated models. Fig. 1 shows an example visualizing the degradation of spatial information in the periphery. Being able to perform a visualization like this in under a second (and thus, thousands in an hour) has several significant applications listed here. As discussed in §4.4, the average running time of 700 ms could be further significantly reduced. As it approaches 33 ms (or 30 fps), the following applications become even more feasible.

- **Behavioral Evaluation of Vision Model:** Testing how well the model captures various properties of peripheral vision requires running experiments with subjects. These experiments need hundreds of foveated images that are sometimes dependent on subject performance, pattern of fixations, and other external variables. FFCN can generate the needed set of foveated images on-the-fly as the subject is performing the experiment.
- **Interface Design:** Explore various graphic user interface design options on the fly by adjusting the fixation point and visualizing the full-field appearance of the design given the fixation point in near real-time. One example of this application is the A/B testing of website designs [10]. An illustrative case study of this testing-based design methodology is presented in Appendix A.
- **Online Experiments:** Ability to generate images on the fly can be used to run online experiments (i.e., on Mechanical Turk) where the subject chooses the fixation point and the image is foveated either client-side (variable performance) or server-side (near real-time).
- **Video Foveation:** Fast image foveation can be applied to individual frames of a video. This is an important step toward producing a model of peripheral vision in real-world viewing. However, there are further modeling challenges like accounting for peripheral encoding of motion and maintaining temporal consistency would need to be added to the architecture in order make video foveation a powerful tool to explore human processing of spatiotemporal visual information.

The contribution, novelty, and validity of this work can be summarized most briefly as follows:

- **Contribution:** Use a deep learning approach to make a model of human vision fast enough to be useful to better understand (1) how human beings see the world, (2) how that knowledge can help build computer vision and graphics systems that can process and generate the visual environment more efficiently, and (3) how that knowledge can help designers more effectively communicate visual information. To the latter two aims, we release the code: <http://lexfridman.com/peripheral>.
- **Novelty:** A model of peripheral vision that is comparable to behaviorally-validated texture synthesis models and yet is 21,000 times faster.
- **Validity:** We provide both a quantitative and qualitative validation of the proposed approach.

## 1.1 Fully Convolutional Networks as End-to-End Generators

Fully convolution neural networks and other generative neural network models have been successfully used in computer vision literature for image segmentation [11, 16], deblurring [26, 27], denoising [4], inpainting [30], and super-resolution [6], artifact removal [7], and general deconvolution [31]. Many of these approaches use end-to-end architectures in that the input to the network is a full image and the output is also a full image (with similar size and dimensions) on which a learned nonlinear operation has been performed. Our work aims to add degradation in a way that is representative of human peripheral vision. As shown in §4.2, this is a highly nonlinear function both in terms of global spatial context and in terms of local texture statistics.

Neural networks have begun to be applied for texture synthesis. Authors in [9] use the 16 convolutional and 5 pooling layers of the VGG-19 network for texture synthesis. In the context of peripheral vision, their work could be viewed as a method for synthesizing individual pooling regions as described in §2. However, to the best of our knowledge, nobody has used neural networks for generating full-field foveated images.

Adding an behaviorally-validated, human-realistic “attentional mechanism” to a generative network is a novel contributions of our work. Recent literature has begun to look at object recognition performance in peripheral vision [28]. In addition to the applications discussed here, CNN-based approaches aiming to mimic human object recognition could benefit from an addition of fully convolutional layers that mimic human peripheral vision losses.

## 1.2 Models of Peripheral Vision

It is well known that the visual system has trouble recognizing peripheral objects in the presence of nearby flanking stimuli, a phenomenon known as crowding (for reviews see: [15, 20, 29]). Fig. 2 shows a classic demonstration. Fixating the central cross, one can likely easily identify the isolated ‘A’ on the left but not the one on the right flanked by additional letters. An observer might see these crowded letters in the wrong order, e.g., ‘BORAD’. They might not see an ‘A’ at all, or might see strange letter-like shapes made up of a mixture of parts from several letters [14]. Move the flanking letters farther from the target ‘A’, and at a certain critical spacing recognition is restored. The critical spacing is approximately 0.4 to 0.5 times the eccentricity (the distance from the center of fixation to the target) for a fairly wide range of stimuli and tasks [3, 18, 19]. Authors in [20] have dubbed this *Bouma’s Law*.

**A                      +                      B O A R D**

Figure 2: A classic example demonstrating the “crowding” effect.

Crowding is likely task-relevant for most real-world visual stimuli and tasks. It has a far greater impact on vision than loss of acuity or color vision, and it is the dominant difference between foveal and peripheral vision [23]. It impacts visual search, object recognition, scene perception, perceptual grouping, shape perception, and reading [20, 24, 25]. The information that makes it through the mechanisms of crowding must suffice to guide eye movements and give us a coherent

view of the visual world [22]. Its pervasive effects mean that we cannot hope to understand much of vision without understanding, controlling for, or otherwise accounting for the mechanisms of visual crowding.

A fair assessment of the current state of vision research is that there exists a dominant theory of crowding. Crowding has been attributed to “excessive or faulty feature integration”, “compulsory averaging”, or “forced texture processing” “pooling”, resulting from of features over regions that grow linearly with eccentricity [2, 14, 15, 17, 20]. Pooling has typically been taken to mean averaging [17] or otherwise computing summary statistics [2, 14] of features within the local region.

## 2 A Statistical Model of Peripheral Vision

Authors in [2] operationalized earlier theories of statistical processing in peripheral vision [14, 17] in terms of measurement of a rich set of texture statistics within local pooling regions that grow linearly with eccentricity, in accord with Bouma’s Law. They used as their candidate statistics those identified by authors in [21], as that set has been successful at describing texture perception (as judged by synthesis of textures that are difficult to discriminate from the original). Authors in [8] generalized this model to synthesize images from local texture statistics computed across the field of view, often referred to as the “V2 model”, as they suggested that these computations might occur in visual processing area V2 in the brain. Authors in [24] have similarly developed full-field synthesis techniques, and refer to the full model as the Texture Tiling Model (TTM). The V2 model and TTM [8, 24] share many features, including the local texture statistics, and overlapping pooling regions that overlap and grow linearly with eccentricity. This paper utilizes the TTM synthesis procedure, so we adopt that terminology.

Mounting evidence supports TTM as a good candidate model for the peripheral encoding underlying crowding; it predicts human performance at peripheral recognition tasks [2, 8, 12, 24], visual search [25, 32], and scene perception tasks [24], and equating those local statistics creates visual metamers [8].

Both the V2 model and TTM are slow to converge, as they must optimize to satisfy a large number of constraints arising from the measured local texture statistics. Authors in [13], on the other hand, have taken a different approach to a related problem. They apply simple image distortions, such as spatial warping, to an image, and have shown that it is surprisingly difficult to tell that anything is wrong away from the fovea. Applying simple image distortions is fast to compute; however, it is not well known what distortions best capture the information available in peripheral vision; this distortion work is not yet as well grounded in terms of being able to predict task performance as TTM and the V2 model. Here the aim is to use deep networks to produce distortions like those introduced by TTM in a more computationally efficient way.

## 3 A Fully Convolutional Model for Foveated Rendering

Given an original undistorted color image  $\mathbf{x}_{i,j}^{\{1,2,3\}}$  of dimension  $h \times w \times 3$  and a spatial weight mask  $\mathbf{x}_{i,j}^{\{4\}}$  of dimension  $h \times w \times 1$ , the task is to produce a foveated image,  $\mathbf{y}$ , of dimension  $h \times w \times 3$ . The fourth channel of  $\mathbf{x}$  captures the global spatial component of the function to be learned as it relates to the fixation point. The mask takes the form:

$$d_{i,j} = \sqrt{(i - f_y)^2 + (j - f_x)^2}$$

$$\mathbf{x}_{i,j,4} = \begin{cases} d_{i,j}, & \text{if } d_{i,j} > d_{\text{fovea}} \\ 0, & \text{otherwise} \end{cases}$$

where  $d_{i,j}$  is the distance of each input pixel to the fixation point  $(f_x, f_y)$  which is assumed to be  $(w/2, h/2)$  in this paper, and  $d_{\text{fovea}}$  is the radius (in pixels) of the foveal region. For the results in §4, the fovea radius is 64 pixels.

The proposed foveated fully convolutional network (FFCN) architecture is based on several components of CNN-based deconvolution approaches [4, 7, 31] and fully convolutional segmentation

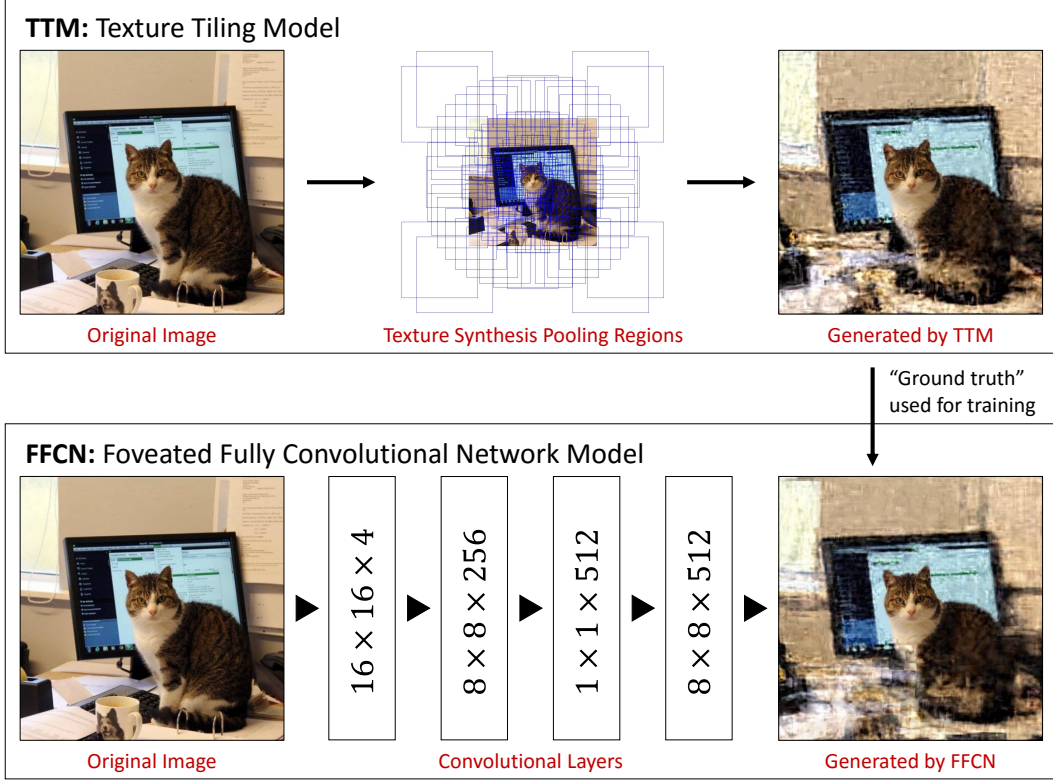


Figure 3: The architecture of the foveated fully convolutional network (FFCN) used to estimate the computationally-costly texture tiling model (TTM). The output of the TTM is used as the ground truth for the end-to-end training of the FFCN.

approaches [11, 16]. A fully convolutional network (FCN) can operate on large image sizes and produce output of the same spatial dimensions. We extend the FCN architecture with the foveation weight mask (see above) and propagate it forward through the biases of each hidden layer in order for the spatial relation with the fixation point to be accounted for in computing the convolution and element-wise sigmoid for each layer:

$$f_k(x) = \tanh(w_k \cdot f_{k-1}(x) + b_k)$$

where  $w_k$  and  $b_k$  are the convolutions and biases at layer  $k$ , respectively.

In our implementation of FFCN, there are 4 convolutional layers  $w_{1,2,3,4}$  with  $w_1$  having 256 kernels of size  $16 \times 16 \times 4$ ,  $w_2$  having 512 kernels of size  $8 \times 8 \times 256$ ,  $w_3$  having 512 kernels of size  $1 \times 1 \times 512$ , and  $w_4$  having 3 kernels of size  $8 \times 8 \times 512$ . The loss function is defined on the whole image pair  $(x, T_i(x))$  where  $T_i(x)$  is the output of the TTM model on image  $x$  given a random seed of  $i$ . For purpose of FFCN, this forms a unique mapping between images, but it should be noted that TTM can generate a very large number of images  $T_i(x), \forall i \in \mathbb{N}$  for a single input image  $x$ , since the number of images that satisfy the statistical constraints imposed by the optimization in TTM are upper-bounded by an exponential function in the number image pixels.

Fig. 3 shows the fully convolutional architecture of FFCN and the TTM method used to generate the foveated image pairs. The key aspect of the former is that the foveation is completed with a single pass through the network.

#### 4 Evaluation of Generative Model

We evaluate two models of foveation. The first is a naive radial blur model known to be a poor visualization of peripheral perception as discussed in §1. However, it is a deterministic model for

which there is a one-to-one mapping between source image and the ground truth. Therefore, it is a good test of whether FFCN can learn a function that is spatially dependent in a global sense on the fixation point. The second is a TTM foveation that has been shown in behavioral experiment to capture some of the more complex characteristics of perception in the periphery (i.e., crowding).

The original undistorted images in this paper are natural scene images selected from the Places dataset [33]. 1,000 images were selected for training the FFCN on both the radial blur model (see §4.1) and the TTM model (see §4.2). Another 1,000 images were used in evaluating FFCN trained on both models. All images were cropped and resized down to  $512 \times 512$  pixels.

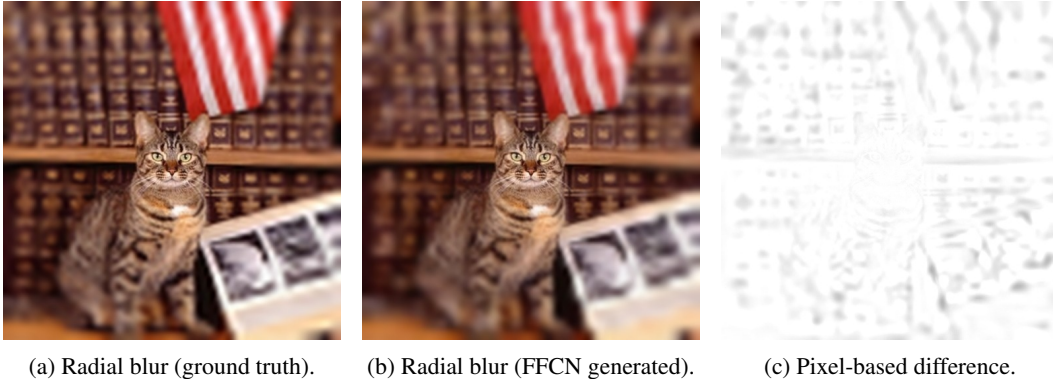


Figure 4: Example output of the radial blur computed directly (a) and learned through the FFCN architecture (b). The pixel-by-pixel difference between the two images (c) shows in black the pixels of the FFCN-generated image that differs from the ground truth.

#### 4.1 Naive Foveation: Training on Radial Blur Model Output

In order to evaluate the ability of FFCN to learn a “foveating” function, we use a Gaussian blur with the standard deviation proportional to the distance away from the fixation. The maximum standard deviation is set to 4 and decreases linearly with distance as both approach zero. Note that this blur is made greater than that needed to mimic human peripheral loss of acuity for the purpose of visualizing the effectiveness of our training procedure. Fig. 4a shows the result of applying the radial blur on one of the images from test set. This blurring function was applied to all 1,000 images in the training set and used as  $y$  in  $(x, y)$  image pairs for training an FFCN network to estimate the radial blur function. Fig. 4b shows the result of running the image in Fig. 1a through the trained network, and Fig. 4c shows the difference between this generated image and the ground truth.

Since radial blur is a deterministic function, we can estimate the pixel error of the images generated by FFCN. The trained model was run on each of the 1,000 images in the test set and achieved an average pixel difference of 2.3. Note that the difference shown in Fig. 4c is inverted intensity-wise for visualization clarity. This result is a quantifiable verification that FFCN can learn a simple radial blurring function, and thus presumably can capture the loss of acuity in the periphery.

#### 4.2 Human-Realistic Foveation: Training on TTM Output

The open question asked by this paper is whether a neural network can learn to degrade peripheral information in an image in a way that is structurally similar to behaviorally validated models like TTM. The results shown for 4 images in Fig. 5 and for 1,000 foveated test images made available online at <http://lexfridman.com/peripheral> indicate that FFCN is able to capture many of the peripheral effects such as crowding and acuity loss. However, evaluating FFCN’s ability to capture the degree of this degradation is difficult. The TTM model has a stochastic component and can produce drastically different local variations while still maintaining consistent texture statistics across its various pooling regions. Furthermore, peripheral vision loses substantial local phase (location) information, an effect well captured by TTM. These two factors make it impossible to evaluate FFCN through pixel-based comparison with the output of TTM. We cannot simply look at the difference between the TTM image and the FFCN output, as we did when evaluating radial blur. Here

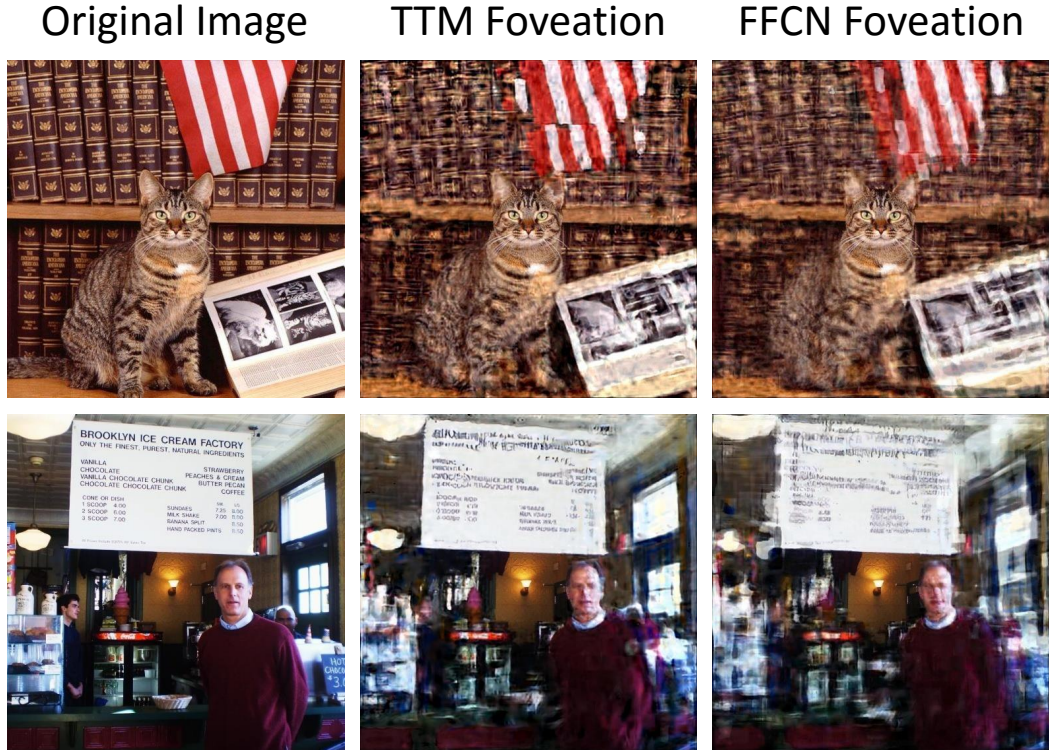


Figure 5: Two examples (rows) from the evaluation dataset showing the original image (column 1), TTM-based foveation of the image (column 2), and FFCN-based foveation of the image (column 3). Unlike the deterministic radial blur function in §4.1, TTM is stochastic and can generate an arbitrary number of foveated images (based on a random number generator seed) from a single source image. Therefore, one should not expect the TTM and FFCN foveations to match pixel by pixel, but rather their synthesis should have similar density and type of information degradation in the periphery.

we show that FFCN and TTM produce qualitatively similar distortions, and evaluate the degree to which the TTM and FFCN outputs match on the statistics explicitly measured by TTM.

In Fig. 5, the first column has the original images, the second column has the TTM foveated images, and the third column has the FFCN Foveation. Visual inspection of these images reveals several key observations. First, the fovea region with the 64 pixel radius is reproduced near-perfectly (the average pixel intensity difference is below 1.9). Second, the results capture a number of known effects of crowding, including the “jumbling” loss of position information, coupled with preservation of many basic features such as orientation and contrast, and dependence of encoding quality on local image contents, including fairly good preservation of homogeneous textured regions [14, 15, 29]. For example, the readability of text in the periphery of the second images is degraded significantly by its nonuniform positional displacement. Third, visual acuity decreases with distance from the fixation point for all 4 images.

### 4.3 Statistical Validation of FFCN

The FFCN model was trained and evaluated based on its ability to mimic, in a meaningful statistic way, the foveated images produced by the TTM model. Therefore, statistical validation of FFCN was performed by comparing its output to TTM output over the same exact pooling regions that were used for the original TTM generation process. In other words, this comparison evaluates the degree to which FFCN is able to mimic the texture feature vector on a region by region basis and thereby mimic the information degradation modeled by TTM.

Fig. 6) shows the per-image difference in the feature vector representing the texture statistics in each pooling region over that image. Each bar represents a unique image. The error in each case is

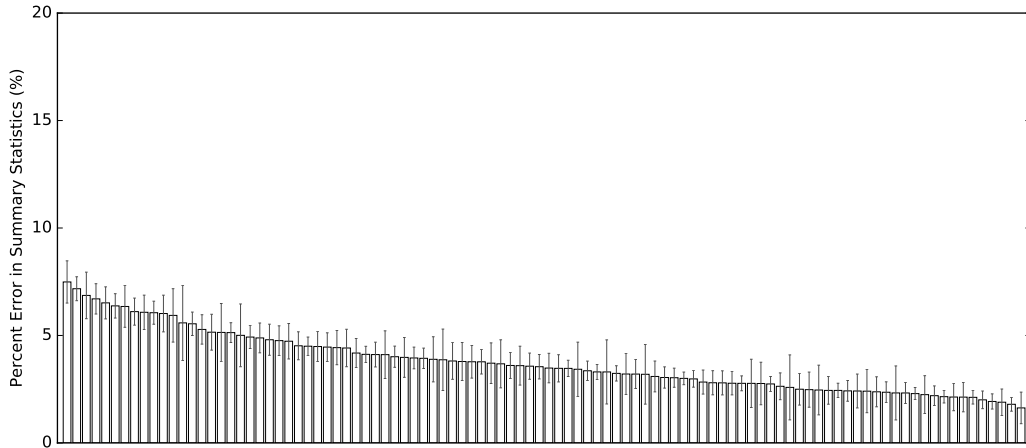


Figure 6: Percent difference (error) between FFCN output and TTM output. The error is computed for each of the 1,000 images in the test dataset and sorted from highest (left) mean error to lowest (right). Only the highest 100 errors are shown in this figure for clarity. The mean and standard deviation of the error are computed for each image by aggregating over each of the values in the summary statistics vector in each of the pooling regions. All mean errors are below 8%.

computed for each of the 1,000 images in the test dataset and sorted from highest (left) mean error to lowest (right). Only the highest 100 errors are shown in the figure for clarity. The mean and standard deviation of the error are computed for each image by aggregating over each of the values in the summary statistics vector in each of the pooling regions. All mean errors are below 8% for the comparison with the TTM output.

#### 4.4 Running Time Performance

TTM hyper-parameters were chosen such that texture synthesis convergence was achieved. For these parameters, the average running time per image was 4.2 hours. The model is implemented in Matlab and given the structure of underlying iterative optimization is not easily parallelizable.

The FFCN architecture was implemented in TensorFlow [1] and evaluated using NVIDIA GTX 980Ti GPU and a 2.6GHz Intel Xeon E5-2670 processor. The average running time per image was 0.7 seconds. That is an over 21,000-fold reduction in running time for foveating an image. There are several aspect of this performance evaluation that indicate the possibility of significant further reductions in running time: (1) no code optimization or architecture pruning was performed, (2) the running time includes I/O read and write operations on a SATA SSD drive, and (3) the GPU and CPU are 2-4 years behind the top-of-the-line affordable consumer hardware.

## 5 Conclusion

We show that a fully convolutional network with a spatial foveating component can learn in an end-to-end way to efficiently estimate the output of a human-realistic model of peripheral vision. We achieve a 4 orders-of-magnitude decrease in running time, from 4.2 hours per image to 0.7 seconds per image. This kind of jump in performance opens the door to a wide variety of applications from interface design to virtual reality to video foveation for studying human behavior in real-world interactions.

**Code, Data, and Future Work** The TTM-generated images used for training are made available online along with the source code at <http://lexfridman.com/peripheral>. Future work will extend the size of the TTM dataset from 1,000 to 100,000 images. This will allow other groups to propose better-performing end-to-end architectures trained on the TTM model. Additionally, future work will pursue the development and evaluation of applications described in §1.



## References

- [1] Martin Abadi, Ashish Agarwal, Paul Barham, Eugene Brevdo, Zhifeng Chen, Craig Citro, Greg S Corrado, Andy Davis, Jeffrey Dean, Matthieu Devin, et al. Tensorflow: Large-scale machine learning on heterogeneous systems. *Software available from tensorflow.org*, 2015.
- [2] Benjamin Balas, Lisa Nakano, and Ruth Rosenholtz. A summary-statistic representation in peripheral vision explains visual crowding. *Journal of vision*, 9(12):13–13, 2009.
- [3] Herman Bouma. Interaction effects in parafoveal letter recognition. *Nature*, 226:177–178, 1970.
- [4] Harold C Burger, Christian J Schuler, and Stefan Harmeling. Image denoising: Can plain neural networks compete with bm3d? In *Computer Vision and Pattern Recognition (CVPR), 2012 IEEE Conference on*, pages 2392–2399. IEEE, 2012.
- [5] Smriti Chawla. Case study lead generation rate shoots up by 232% with masthead changes, 2013. [Online; accessed 10-August-2016].
- [6] Chao Dong, Chen Change Loy, Kaiming He, and Xiaoou Tang. Learning a deep convolutional network for image super-resolution. In *Computer Vision–ECCV 2014*, pages 184–199. Springer, 2014.
- [7] David Eigen, Dilip Krishnan, and Rob Fergus. Restoring an image taken through a window covered with dirt or rain. In *Proceedings of the IEEE International Conference on Computer Vision*, pages 633–640, 2013.
- [8] Jeremy Freeman and Eero P Simoncelli. Metamers of the ventral stream. *Nature neuroscience*, 14(9):1195–1201, 2011.
- [9] Leon A Gatys, Alexander S Ecker, and Matthias Bethge. Texture synthesis and the controlled generation of natural stimuli using convolutional neural networks. *arXiv preprint arXiv:1505.07376*, 2015.
- [10] Bruce Hanington and Bella Martin. *Universal methods of design: 100 ways to research complex problems, develop innovative ideas, and design effective solutions*. Rockport Publishers, 2012.
- [11] Kai Kang and Xiaogang Wang. Fully convolutional neural networks for crowd segmentation. *arXiv preprint arXiv:1411.4464*, 2014.
- [12] Shaiyan Keshvari and Ruth Rosenholtz. Pooling of continuous features provides a unifying account of crowding. *Journal of vision*, 16(3):39–39, 2016.
- [13] Jan Koenderink, Whitman Richards, and Andrea J van Doorn. Space-time disarray and visual awareness. *i-Perception*, 3(3):159–165, 2012.
- [14] Jerome Y Lettvin. On seeing sidelong. *The Sciences*, 16(4):10–20, 1976.
- [15] Dennis M Levi. Crowdingan essential bottleneck for object recognition: A mini-review. *Vision research*, 48(5):635–654, 2008.
- [16] Jonathan Long, Evan Shelhamer, and Trevor Darrell. Fully convolutional networks for semantic segmentation. In *Proceedings of the IEEE Conference on Computer Vision and Pattern Recognition*, pages 3431–3440, 2015.
- [17] Laura Parkes, Jennifer Lund, Alessandra Angelucci, Joshua A Solomon, and Michael Morgan. Compulsory averaging of crowded orientation signals in human vision. *Nature neuroscience*, 4(7):739–744, 2001.
- [18] Denis G Pelli, Najib J Majaj, Noah Raizman, Christopher J Christian, Edward Kim, and Melanie C Palomares. Grouping in object recognition: The role of a gestalt law in letter identification. *Cognitive Neuropsychology*, 26(1):36–49, 2009.
- [19] Denis G Pelli, Melanie Palomares, and Najib J Majaj. Crowding is unlike ordinary masking: Distinguishing feature integration from detection. *Journal of vision*, 4(12):12–12, 2004.
- [20] Denis G Pelli and Katharine A Tillman. The uncrowded window of object recognition. *Nature neuroscience*, 11(10):1129–1135, 2008.
- [21] Javier Portilla and Eero P Simoncelli. A parametric texture model based on joint statistics of complex wavelet coefficients. *International Journal of Computer Vision*, 40(1):49–70, 2000.

- [22] Martin Rolfs, Donatas Jonikaitis, Heiner Deubel, and Patrick Cavanagh. Predictive remapping of attention across eye movements. *Nature neuroscience*, 14(2):252–256, 2011.
- [23] Ruth Rosenholtz. Capabilities and limitations of peripheral vision. *Annual Review of Vision Science*, 2(1), 2016.
- [24] Ruth Rosenholtz, Jie Huang, and Krista A Ehinger. Rethinking the role of top-down attention in vision: effects attributable to a lossy representation in peripheral vision. *Frontiers in Psychology*, 2012.
- [25] Ruth Rosenholtz, Jie Huang, Alvin Raj, Benjamin J Balas, and Livia Ilie. A summary statistic representation in peripheral vision explains visual search. *Journal of Vision*, 12(4):14–14, 2012.
- [26] Christian J Schuler, Michael Hirsch, Stefan Harmeling, and Bernhard Schölkopf. Learning to deblur. *arXiv preprint arXiv:1406.7444*, 2014.
- [27] Jian Sun, Wenfei Cao, Zongben Xu, and Jean Ponce. Learning a convolutional neural network for non-uniform motion blur removal. In *Computer Vision and Pattern Recognition (CVPR), 2015 IEEE Conference on*, pages 769–777. IEEE, 2015.
- [28] Panqu Wang and Garrison Cottrell. Modeling the contribution of central versus peripheral vision in scene, object, and face recognition. *arXiv preprint arXiv:1604.07457*, 2016.
- [29] David Whitney and Dennis M Levi. Visual crowding: A fundamental limit on conscious perception and object recognition. *Trends in cognitive sciences*, 15(4):160–168, 2011.
- [30] Junyuan Xie, Linli Xu, and Enhong Chen. Image denoising and inpainting with deep neural networks. In *Advances in Neural Information Processing Systems*, pages 341–349, 2012.
- [31] Li Xu, Jimmy SJ Ren, Ce Liu, and Jiaya Jia. Deep convolutional neural network for image deconvolution. In *Advances in Neural Information Processing Systems*, pages 1790–1798, 2014.
- [32] Xuetao Zhang, Jie Huang, Serap Yigit-Elliott, and Ruth Rosenholtz. Cube search, revisited. *Journal of vision*, 15(3):9–9, 2015.
- [33] Bolei Zhou, Agata Lapedriza, Jianxiong Xiao, Antonio Torralba, and Aude Oliva. Learning deep features for scene recognition using places database. In *Advances in neural information processing systems*, pages 487–495, 2014.

## A Application Case Study: A/B Testing of Design Layouts



(a) Old design snapshot (original image).



(b) Old design snapshot (image foveated on “S” in “Serving”).



(c) New design snapshot (original image).



(d) New design snapshot (image foveated on “S” in “Serving”).

Figure 7: Example “foveated” image. Given an original image (a), the foveated image provides a visualization of human-realistic perception of the information available from a single glance (b). This particular visualization assumes that the two subfigures are 14.2 inches away from the observer on a printed page (2.6 inches in height and width) and the observers eyes are fixated on the “S” in “Serving” (middle left).

A case study of a shipping website describes a significant increase in customers requesting quotes [5] based on a redesign shown in Fig. 7. FFCN can be effectively used by a designer, in this case, to reveal the effects of crowding when the user’s eyes go to the first word of the most relevant content. Keeping a first-time visitor in mind, a designer may make the following quick observations using the FFCN output for the first design in Fig. 7:

- You might have a chance of recognizing a truck.
- You can tell where the logo is, probably.
- It looks like the background is a scene of some sort.
- There’s some black, and blue below it, and an orange circle.
- Probably the black at least has text on it.
- The top light line is probably a menu bar. The model suggests you can tell that when fixating so far away. The gray bar in the middle of the page also might be a navigation bar. Both of these are important things for the user to get at a glance.

Similarly, a designer may make the following quick observations using the FFCN output for the second design in Fig. 7:

- Clearly text against the blue background, clearly smaller text below the bigger text.
- Clear where the logo is. Clear the top bar is likely navigation. Middle bar, too (possibly even more clear than above because of higher contrast).
- Red rectangle of some sort is clear. Based on higher level knowledge (not possible above) this is probably a button.

With the main button in mind, a designer may use the FFCN output to conclude that the button in both designs is “clear” in the “salient” sense. In the case of the second design, the clarity is somewhat better because obviously not part of a scene, but the button in the first design is also pretty good. However, once you get past the visual aspects, the second design’s button is sufficiently preserved that an observer can use higher level knowledge to guess that it is in fact a button. This kind of reasoning process may be beneficial to a designer for arriving at the more effective design prior to engaging to the kind of A/B testing described in [5].